Published in final edited form as:
Biol Psychiatry. 2009 June 1; 65(11): 927–934. doi:10.1016/j.biopsych.2009.01.027.

Beta Amyloid in Alzheimer's Disease: Increased Deposition in Brain Is Reflected in Reduced Concentration in Cerebrospinal Fluid

Timo Grimmer[1], **Matthias Riemenschneider**[1,3], **Hans Förstl**[1], **Gjermund Henriksen**[2], **William E. Klunk**[4], **Chester A. Mathis**[5], **Tohru Shiga**[2,6], **Hans-Jürgen Wester**[2], **Alexander Kurz**[1], and **Alexander Drzezga**[2]

1 *Department of Psychiatry and Psychotherapy, Klinikum rechts der Isar der Technischen Universität München, Munich*

2 *Department of Nuclear Medicine, Klinikum rechts der Isar der Technischen Universität München, Munich*

3 *Department of Psychiatry and Psychotherapy, Universitätsklinikum, Homburg/Saar, Germany*

4 *Department of Psychiatry, Western Psychiatric Institute & Clinic, University of Pittsburgh, Pittsburgh, Pennsylvania*

5 *Department of Radiology, University of Pittsburgh, Pittsburgh, Pennsylvania*

6 *Department of Nuclear medicine, School of Medicine, Hokkaido University, Hokkaido, Japan*

Abstract

Background—A decreased concentration of beta amyloid (1–42) (Aβ42) has consistently been found in the cerebrospinal fluid (CSF) of patients with Alzheimer's disease (AD) and is considered a diagnostic biomarker. However, it is not clear to which extent CSF Aβ42 levels are reflective of cerebral pathology in AD. The aim of the study was to determine the association between cerebral amyloid plaque load, as measured by means of the positron emission tomography (PET) tracer carbon-11-labeled Pittsburgh Compound B ([^{11}C]PiB) and CSF Aβ42 in AD.

Methods—A group of 30 patients with probable AD, as defined by established clinical criteria and by an AD-typical pattern of tracer uptake in fluorine-18-labeled fluorodeoxyglucose ([^{18}F]FDG) PET, were included. In all patients, [^{11}C]PiB PET and CSF analysis were performed. The association between amyloid load and CSF Aβ42 levels was examined in three different ways: by linear regression analysis using an overall [^{11}C]PiB value for the entire cerebrum, by correlation analyses using [^{11}C]PiB measurements in anatomically defined regions of interest, and by voxel-based regression analyses.

Results—All patients showed a positive [^{11}C]PiB scan demonstrating amyloid deposition. Linear regression analysis revealed a significant inverse correlation between the overall [^{11}C]PiB uptake and CSF Aβ42 levels. Voxel-based regression and regional correlation analyses did not attain statistical significance after correction for multiple comparisons. Numerically, correlation coefficients were higher in brain regions adjacent to CSF spaces.

Address reprint requests to Timo Grimmer, M.D., Klinik und Poliklinik für Psychiatrie und Psychotherapie, Klinikum rechts der Isar, Technische Universität München, Möhlstr. 26, 81675 München, Germany; E-mail: E-mail: t.grimmer@lrz.tum.de.

Supplementary material cited in this article is available online.

Conclusions—The study demonstrates a moderate linear negative association between cerebral amyloid plaque load and CSF Aβ42 levels in AD patients in vivo and suggests possible regional differences of the association.

Keywords

Alzheimer's disease; Aβ42; [^{11}C]PiB; CSF; [^{18}F]FDG; positron emission tomography; Pittsburgh Compound B

The characteristic neuropathological features of Alzheimer's disease (AD) are senile plaques (SP) and neurofibrillary tangles (NFT) in conjunction with loss of neurons and synapses (1, 2). The major constituent of SP is amyloid beta protein (Aβ), particularly the rapidly aggregating 42 amino acid variant (Aβ42) (3). A decreased concentration of Aβ42 has consistently been found in the cerebrospinal fluid (CSF) of AD patients as compared with cognitively unimpaired age-matched subjects. The observation that decreased levels of Aβ42 are already present at very early clinical (4,5) and even presymptomatic (6) stages of AD is consistent with the neuropathological finding that amyloid deposition represents an early event in the course of AD that may precede the onset of symptoms by decades (1). Consequently, CSF Aβ42 levels are regarded as a diagnostic biomarker (7–10) for early and reliable diagnosis of AD.

However, the mechanisms leading to reduced levels of CSF Aβ42 in AD are unclear. It has been hypothesized that low levels are a result of sequestration of the peptide in the brain and reduced clearance into the CSF (11). Evidence supporting this view is provided by the postmortem finding that higher SP counts are associated with significantly lower Aβ42 levels (12) and by longitudinal studies demonstrating a significant decrease of CSF Aβ42 over time (13). However, since low CSF Aβ42 concentrations are also found in other dementias that do not show plaque formation, such as Creutzfeldt-Jakob disease, amyotrophic lateral sclerosis, and multiple system atrophy (14), and since recent evidence suggests that soluble Aβ42 oligomers may reduce γ-secretase activity (15), reduced neuronal production of Aβ42 is another possibility (16). An in vivo marker of amyloid deposition measured in close temporal relationship to CSF Aβ42 assessments might be helpful to obtain additional information on the association between amyloid in the brain and in the CSF.

Recently, the tracer carbon-11-labeled Pittsburgh Compound B ([^{11}C]PiB) has become available for the in vivo imaging of cerebral amyloid plaques using positron emission tomography (PET) (17). In vitro studies have demonstrated that Pittsburgh Compound B (PiB) binds to different kinds of cerebral Aβ, including plaque and nonplaque deposits as well as vascular Aβ, while binding to other types of protein aggregations such as neurofibrillary tangles or Lewy bodies is minimal (18–20). Accordingly, in vivo studies of patients with AD have consistently demonstrated an increased cerebral uptake of [^{11}C]PiB (17,21–23). In a recent study, an analysis of cerebral [^{11}C]PiB binding and CSF Aβ42 levels has been performed in a small group of healthy subjects and patients with dementia (21). In this study, all of four AD patients showed positive [^{11}C]PiB binding and low CSF Aβ42 levels, whereas 15 out of 18 healthy individuals exhibited negative [^{11}C]PiB binding and high CSF Aβ42 levels. The quantitative association between [^{11}C]PiB binding and CSF Aβ42 concentration within AD was not examined.

The primary aim of the present study was to determine the association between cerebral amyloid plaque load as measured by [^{11}C]PiB-PET and Aβ42 in the CSF within a larger group of patients with probable AD as defined by established clinical criteria and by an AD-typical pattern in fluorine-18-labeled fluorodeoxyglucose ([^{18}F]FDG) PET. The secondary aim was to explore possible regional differences of the association pattern.

Methods and Materials

Patient Recruitment, Inclusion and Exclusion Criteria

Patients were recruited from the research outpatient unit for cognitive disorders at the Department of Psychiatry, Klinikum rechts der Isar, Technische Universitaet Muenchen, Munich, Germany. They had been referred for the diagnostic evaluation of cognitive impairment by general practitioners, neurologists, psychiatrists, or other institutions, and underwent a standardized diagnostic procedure.

The diagnostic work-up included an interview with the patient and an informant; medical, psychiatric, and neurological examinations; neuropsychological evaluation including the Mini Mental State Examination (MMSE) (24); a routine laboratory screen; and apolipoprotein E (APOE) genotyping. The severity of cognitive impairment was rated on the Clinical Dementia Rating (CDR) scale, and the CDR sum of boxes (CDR SOB) (25) was calculated. Cranial magnetic resonance imaging (MRI) was performed to assess structural brain abnormalities. Cranial [^{18}F]FDG PET was used to measure cerebral metabolism, and [^{11}C]PiB PET was used to assess amyloid plaque burden.

The study protocol was approved by the institutional review board (IRB) and by radiation protection authorities.

All study participants met National Institute of Neurological and Communicative Diseases and Stroke-Alzheimer's Disease and Related Disorders Association (NINCDS-ADRDA) diagnostic criteria for probable Alzheimer's disease (26). Patients with mild to moderate dementia were included. Furthermore, [^{18}F]FDG PET findings typical for AD were required for inclusion, i.e., hypometabolism in the temporoparietal and posterior cingulate cortex with relative sparing of the primary sensomotor cortex on visual inspection (27).

Patients were not included if they met diagnostic criteria for other neurological or psychiatric disorders, including Parkinson's disease, normal pressure hydrocephalus, progressive nuclear palsy, or major depression. Patients were also excluded if they showed any major abnormalities on MRI, such as brain infarcts or extensive leucoencephalopathy. Moreover, patients with [^{18}F]FDG PET findings not typical for AD were excluded. National Institute of Neurological Disorders and Stroke-Association Internationale pour la Recherché et l'Enseignement en Neurosciences (NINDS-AIREN) criteria were used to exclude vascular dementia (28). Furthermore, patients with other possible causes of cognitive impairment such as psychotropic medication (e.g., antidepressants, antipsychotics), substance misuse, or major abnormalities in routine blood testing were not enrolled.

Laboratory Screen and APOE Genotyping

Routine blood screening included a standard serologic chemistry group, full blood cell count, blood glucose, vitamin B12 and folic acid levels, and thyroid hormone levels, as well as serological tests for syphilis and Lyme borreliosis. Apolipoprotein E genotype was determined following a standardized protocol using a polymerase chain reaction (PCR)-based assay that simultaneously utilizes two distinct restriction enzymes (29).

Lumbar Puncture

Cerebrospinal fluid (5 to 8 mL) was collected in sterile polypropylene tubes and gently mixed to avoid gradient effects. In native CSF, routine chemical parameters were determined. These parameters included cell count, as well as glucose and lactate measurement, total protein content, CSF/serum ratio of albumin and immunoglobulin G, and a screening for oligoclonal bands. The remaining CSF was centrifuged for 10 minutes at 4000*g*, and aliquots were stored

at −80°C for subsequent Aβ42 measurement. Cerebrospinal fluid Aβ42 concentrations were measured in duplicate by enzyme-linked immunosorbent assay (ELISA) (Innogenetics, Zwijndrecht, Belgium) (30). Beta amyloid [1-42] concentrations above 643 ng/L were considered as normal (7).

Brain Imaging

Three imaging procedures were performed in each patient within 1 month of the initial visit.

MRI—Patients underwent examination on a Siemens 1.5 Tesla Magnetom Symphony (Siemens AG, Erlangen, Germany) using a standardized imaging protocol that consisted of a three-dimensional (3-D) T1 dataset (repetition time [TR] 1520 msec, echo time [TE] 3.93 msec, 256 × 256 matrix, flip angle 15°, 1 mm slices), axial T2-weighted turbo spin-echo images (TR 4510 msec, TE 104 msec, 19 slices, voxel dimensions .6 × .5 × 6.0 mm), coronal T1-weighted spin-echo images (TR 527 msec, TE 17 msec, 19 slices, voxel dimensions .9 × .9 × 6.0 mm), and T2-weighted gradient-echo images (TR 725 msec, TE 29 msec, 19 slices, voxel dimensions .7 × .7 × 6.0 mm). In addition to visual assessment, MRI data of each patient were automatically spatially normalized to the MRI Montreal Neurological Institute (MNI) template in SPM2 (Wellcome Trust, London, United Kingdom) (31) to obtain warping parameters for later normalization of individual [^{11}C]PiB data.

[^{18}F]FDG PET—Subjects received 370 MBq [^{18}F]FDG at rest with eyes closed. Patients were positioned with the head parallel to the canthomeatal line within the gantry. Thirty minutes after injection, PET imaging was performed under standard resting condition (eyes closed in dimmed ambient light) using a Siemens ECAT HR+ PET scanner (CTI, Knoxville, Tennesse), as published previously (32). A sequence of one frame of 10 minutes and two frames of 5 minutes was started and later summed into a single frame. Image data were acquired in 3-D mode with a total axial field of view of 15.5 cm. A transmission scan was acquired after completion of the emission scan for attenuation correction.

[^{11}C]PiB PET—This part of the examination was performed on the same scanner and followed a standardized protocol (33). All patients were injected with 370 MBq [^{11}C]PiB at rest. At 40 minutes postinjection, three 10-minute frames were started and later summed into a single frame (40–70 minutes). Acquisition was carried out in 3-D mode, and a transmission scan was carried out to allow for later attenuation correction. Following image reconstruction, correction of dead time, scatter and attenuation correction, and generation of standard uptake value ratio (SUVR) 40 minute to 70 minute images, spatial normalization was carried out in SPM2. The [^{11}C]PiB data were first coregistered to each individual's volumetric MRI and then automatically spatially normalized to the T1 MRI MNI template in SPM2 using warping parameters derived from the individual MRI normalization performed previously (34,35).

Statistical Analysis

For the primary analysis, we calculated the standardized regression coefficient beta between [^{11}C]PiB uptake and CSF Aβ42, controlling for APOE genotype, duration of disease, and age. Two anatomical regions of interest (ROI) were defined, one covering the entire cerebral gray matter and the other the cerebellar vermis as a reference region, using an established predefined template (36). Mean standard uptake volume (SUV) values were calculated for the 95% of voxels that showed the highest uptake values for each ROI (37). Cerebral to cerebellar vermis ratios were calculated for each patient separately to rule out artifacts due to between-subjects differences in tracer uptake (35). A linear regression analysis was calculated to examine the association between [^{11}C]PiB cerebrum/vermis uptake ratio and the concentration of CSF Aβ42 (in ng/L), including tracer uptake as dependent variable and CSF Aβ42 as independent variable. Apolipoprotein E genotype and duration of disease, as well as age were included as

possibly confounding variables. A stepwise selection of variables was chosen (*F* value for inclusion ≤ .05; *F* value for exclusion ≥.1). These analyses were calculated using SPSS 15.0 software (SPSS Inc., Chicago, Illinois).

Secondary analyses were conducted to identify a possible regional variability in the strength of the association between [^{11}C]PiB uptake and CSF Aβ42. We performed 1) a correlation analysis based on 90 anatomically defined ROI, 2) a voxel-based regression analysis, and 3) a voxel-based regression analysis using correction of partial volume effect (PVE).

The brain was divided into 90 anatomically defined ROIs covering the cortex and subcortical gray matter of the cerebrum using an established predefined template (36). Cerebral to cerebellar vermis ratios were calculated as described above.

A voxel-based statistical parametric regression analysis using SPM2 (38) between [^{11}C]PiB uptake and CSF Aβ42 was performed. As before, the values of all pixels in each patient's [^{11}C]PiB scan were normalized to the cerebellar vermis (36,37) and images were smoothed (Gaussian kernel of 10 × 10 × 10 mm). A significance threshold of .01 was applied.

To explore a potential influence of regional cortical atrophy on the association between [^{11}C] PiB uptake and CSF Aβ42, a correction of [11C]PIB PET data for partial volume effects was carried out with an algorithm implemented in the PMOD software package (PMOD Technologies Ltd., Adliswil, Switzerland). Following coregistration of individual MRI and PET data, a segmentation of the magnetic resonance (MR) information into gray and white matter was carried out. The segmented MR data were then used for PVE correction of the PET data of every subject. Four patients were excluded from the analysis because of failure of the MR segmentation process. Subsequently, all PVE-corrected PET data sets were stereotactically normalized to the standard template and voxel-based statistical analysis was carried out following the identical strategy as described above.

Results

Patients

Thirty patients were included in the study. Demographic and clinical information, as well as results of CSF Aβ42 measurement are shown in Table 1. Patients with a broad range of clinical severity, including very mild to moderate dementia, were included. Five patients who scored unimpaired on the MMSE (28–30 points) exhibited cognitive deficits in neuropsychological testing; all five showed deficits in verbal memory, four had language deficits, one had constructional apraxia, and one had deficits in executive functions.

All patients showed a pattern of hypometabolic areas on [^{18}F]FDG PET that was consistent with the diagnosis of AD. The average time interval between [^{11}C]PiB PET examination and lumbar puncture was 29 ± 41 days.

Sixteen of the 30 patients were included in a study addressing the association between clinical severity and [^{11}C]PiB uptake (35). Four of these 16 patients were part of a patient sample comparing AD and semantic dementia with [^{18}F]FDG and [^{11}C]PiB PET (22).

Visual Inspection of [^{11}C]PiB Scans

On visual analysis, all patients showed an AD-typical tracer uptake in the brain, as previously described (17,22). In a few patients, tracer uptake was unevenly distributed and low in several areas. No patient showed a [^{11}C]PiB-negative scan.

Primary Analysis: Association Between [^{11}C]PiB Uptake and CSF Aβ42

The variable selection in the linear regression analysis using [^{11}C]PiB cerebrum/vermis uptake ratio as dependent variable included CSF Aβ42 as independent variable.

Duration of disease, age, and APOE genotype were excluded during variable selection, i.e, those variables were not significantly associated with CSF Aβ42 concentrations in this sample.

The standardized regression coefficient beta was −0,478 with a p value of .01, indicating an inverse association between [^{11}C]PiB cerebrum/vermis uptake ratio and CSF Aβ42. The scatter plot of this analysis is shown in Figure 1.

Secondary Analyses: Regional Variability of the Strength of the Association

Associations between [^{11}C]PiB uptake in the 90 anatomically defined ROIs and CSF Aβ42 are shown in Supplement 1, including Pearson's correlation coefficient r and p value (uncorrected for multiple comparisons). Inverse associations were found in all ROIs. None of the associations, however, survived Bonferroni's correction for multiple comparisons. Numerically, correlation coefficients were particularly high ($r < -.360$, $p < .05$ uncorrected for multiple comparisons) in ROIs adjacent to the brain ventricles (gyrus cinguli bilaterally, precuneus bilaterally, nucleus caudatus bilaterally, thalamus bilaterally, left gyrus calcarinus, hippocampus bilaterally, left gyrus lingualis, gyrus olfactorius bilaterally, gyrus parahippocampalis bilaterally). In addition, strong associations ($r < -.360$, $p < .05$) between [^{11}C]PiB and CSF Aβ42 were identified in several ROIs close to the basal parts of the external CSF spaces (frontobasal: left gyrus rectus, lateral and mesial orbital parts of middle gyrus frontalis bilaterally, left orbital part of gyrus frontalis superior, triangular part of gyrus frontalis bilaterally; occipitobasal: left gyrus lingualis, gyrus fusiformis bilaterally, left gyrus calcarinus, left gyrus occipitalis inferior, left gyrus temporalis inferior).

Representative scatterplots of these analyses are shown in Figure 2.

The voxel-based regression analysis revealed a widespread pattern of significant associations between [^{11}C]PiB uptake and CSF Aβ42. Association maxima were found in the same regions where correlation coefficients numerically were highest in the previously described ROI approach.

Local maxima of associations are provided with the respective standard stereotactic coordinates in Talairach space (39), Z scores, corresponding anatomical regions, and Brodmann areas using Talairach Client (University of Texas Health Science Center, San Antonio, Texas), and p values in Supplement 2. In Figure 3, the surface projections and representative overlays on averaged T2-weighted MR images of the associations are shown, the latter visualizing the stronger associations in cerebral regions in close vicinity to the CSF.

The PVE-corrected voxel-based regression analysis that controls for possible artifacts due to cortical atrophy only detects cortical associations because of the MR gray matter segmentation process. It revealed a widespread pattern of significant associations between [^{11}C]PiB uptake and CSF Aβ42. The cortical associations did not show major differences as compared with the voxel-based regression analysis uncontrolled for PVE. The result confirms the validity of the associations found in the previous analysis. Local maxima are provided in Supplement 3. In Figure 4, the surface projections of the associations are shown.

Discussion

The primary analysis revealed that [^{11}C]PiB uptake ratio was associated with CSF Aβ42 levels within the group of patients diagnosed with probable Alzheimer's disease. All patients had a

positive [^{11}C]PiB scan demonstrating amyloid deposition but there was interindividual variability of tracer uptake, and a significant inverse linear correlation between the two measures was observed. This finding may be regarded as an in vivo parallel of a postmortem investigation that showed that the number of neuritic plaques in the neocortex and in the hippocampus was strongly associated with lower levels of Aβ42 obtained from the brain ventricles at autopsy (12). It should be mentioned that another investigation that related CSF Aβ42 measured during life and SP numbers (40) determined at autopsy according to the Braak staging did not find this association, possibly because the time interval between CSF collection and brain autopsy was very long, at least in some subjects. In the present study, the average interval between CSF analysis and cerebral [^{11}C]PiB did not exceed 60 days.

The present study provides complementary information to a recent in vivo study that also addressed [^{11}C]PiB uptake and CSF Aβ42 levels (21). In that study, a heterogeneous population had been examined, composed of 4 AD patients, 2 patients with non-AD dementia, and 18 cognitively healthy control subjects. The time interval between [^{11}C]PiB PET and Aβ42 CSF measurement was 1 to 2 years. The authors were able to identify two nonoverlapping groups: a group with positive [^{11}C]PiB binding and low CSF Aβ42 levels, which included all AD patients, and a group with negative [^{11}C]PiB binding and normal CSF Aβ42 levels, which comprised most healthy subjects. Due to the small sample size, the association between CSF Aβ42 levels and [^{11}C]PiB binding was not determined in the patient groups.

The present study extends these results by demonstrating a negative linear relationship between [^{11}C]PiB uptake and CSF Aβ42 concentration in a patient population that was exclusively composed of AD subjects, all of whom showed a positive [^{11}C]PiB PET scan. This finding is compatible with the hypothesis that low levels of CSF Aβ42 in AD are a result of sequestration of Aβ42 in the brain and reduced clearance into the CSF. It is also consistent with the negative feedback hypothesis that amyloid deposits decrease amyloid production and lead to reduced CSF Aβ42 levels.

The secondary analyses that addressed the possible regional variability in the strength of the association between [^{11}C]PiB uptake and CSF Aβ42 did not attain statistical significance after correction for multiple comparisons.

Therefore, no firm conclusions can be made. However, on the basis of the regional differences between correlation coefficients in the ROI analysis and in the voxel-based regression, we speculate that the strength of the association might not be evenly distributed throughout the brain. In two secondary analyses, the relationship between amyloid deposition and CSF Aβ42 appeared to be stronger in gray matter regions that are located in the vicinity of the brain ventricles and the basal parts of the external CSF spaces. This suggests that the levels of Aβ42 in the CSF may particularly reflect the AD pathology in brain areas near the ventricular system.

The possible regional differences and the moderate correlation between [^{11}C]PiB uptake and CSF Aβ42 could be of relevance for the investigation of antiamyloid therapeutic strategies. Our data suggest that CSF Aβ42 might provide information about AD pathology in brain areas that are adjacent to the ventricular system, whereas amyloid PET tracers might map the entire cerebral amyloid pathology. Taking into account the imperfect match between the two measures, the contribution of both techniques may be considered in evaluating the efficacy of antiamyloid therapeutic agents.

In addition, the voxel-based regression analysis suggested that negative correlation between [^{11}C]PiB uptake and CSF Aβ42 also occurs in white matter areas. It is not surprising to find an association between the two measures there, since amyloid plaque deposition in white matter has been described in AD, particularly at more advanced stages (41), and PiB binding in the

white matter has been demonstrated (19). It cannot be ruled out that some unspecific [^{11}C]PiB uptake occurred in the white matter. A possible explanation for the inverse correlation between [^{11}C]PiB uptake and CSF Aβ42 in the white matter would be an impaired perivascular drainage pathway (42).

If indeed [^{11}C]PiB uptake and CSF Aβ42 were more closely associated with one another in gray and white matter close to CSF spaces, this would be compatible with animal studies showing location-dependent differences in the removal of Aβ42 from the brain (43,44). According to these studies, Aβ42 generated in regions close to CSF spaces is directly drained into this fluid compartment, so that tissue levels and CSF concentrations could be tightly linked. On the other hand, Aβ42 produced in CSF-remote regions is cleared through other channels, including the perivascular interstitial fluid channels that follow the cortical arteries. It is tempting to speculate that this pathway could be associated with amyloid angiopathy.

The regional pattern of the associations between [^{11}C]PiB uptake and CSF Aβ42 is somewhat different from the areas of highest [^{11}C]PiB uptake. To rule out the influence of possible normalization artifacts due to cerebral atrophy on the association, we repeated the voxel-based analysis using a PVE correction procedure. The cortical association pattern still demonstrates the widespread association pattern found in the previous analysis. Thus, the cortical associations are not an effect of cerebral atrophy. The PVE approach was not useful for exploring the associations identified in subcortical and white matter areas, because the included MR segmentation preprocess does not include these structures. Thus, we cannot rule out that the associations in these areas are partially influenced by effects of cerebral atrophy.

The present study has several limitations. First, the clinical diagnosis of AD was not confirmed by postmortem examination, and misclassification of patients as AD might have influenced the strength of the association. However, patients were only enrolled if they showed AD-typical findings on [^{18}F]FDG PET. In a few patients, due to uneven uptake of [^{11}C]PiB in the brain and low uptake in several areas, the whole cerebrum/cerebellar vermis ratio was only mildly increased. Second, the design was cross-sectional, and the association may be due to a selection bias. Therefore, the inverse relationship between [^{11}C]PiB uptake and CSF Aβ42 needs to be confirmed in a longitudinal study. Third, the sample size was relatively small. A study in a larger patient sample would be of great interest to determine whether there is a regional variability of the association between [^{11}C]PiB uptake and CSF Aβ42 depending on closeness to CSF spaces and to identify potential modifiers of the association such as APOE genotype. Fourth, all [^{11}C]PiB data in the current study were normalized to the cerebellar vermis, which was used as a reference region. As a consequence, an association of CSF Aβ42 with amyloid plaque deposition in the cerebellar vermis would have been overlooked. However, amyloid plaques only appear in the cerebellum at the most advanced stages of AD (2).

The present study was not designed to compare the diagnostic accuracy of [^{11}C]PiB uptake and CSF Aβ42. The study population was relatively small and highly selected. Moreover, it was exclusively composed of AD patients and did not contain control subjects. We would like to point out, however, that 5 out of 30 patients had CSF Aβ42 levels in the normal range, whereas only 2 patients showed low [^{11}C]PiB uptake. On the basis of this observation, one might speculate that in a larger sample of patients and cognitively healthy control subjects, [^{11}C]PiB uptake might prove to be a more sensitive marker of AD than CSF Aβ42, unless it produces a higher number of false-positive results.

Regarding the two patients with relatively low [^{11}C]PiB uptake, the question could be raised whether these individuals might have been misdiagnosed as AD and, in fact, suffer from dementia with Lewy bodies (DLB). We cannot rule out this possibility, because patients with DLB may show moderate [^{11}C]PiB uptake (45,46) and neuropathological verification of our

clinical diagnosis is not presently available. However, the [^{18}F]FDG PET finding for both patients was typical for AD and did not show evidence of occipital hypometabolism. Further, both patients did not exhibit the clinical core symptoms of DLB (47). Therefore, we assume that the relatively low [^{11}C]PiB uptake was a reflection of the mild severity of dementia in these patients. Another explanation is that the low [^{11}C]PiB uptake was due to a measurement error.

In conclusion, we found a significant inverse linear association between [^{11}C]PiB uptake and CSF Aβ42 in patients with probable AD. Thus, the concentration of Aβ42 in the CSF may not only be a marker that qualitatively discriminates between individuals with AD and healthy control subjects but also a quantitative measure of β-amyloid load within AD, although the strength of the correlation is only moderate. In addition, our observations point to the possibility that the association between [^{11}C]PiB uptake and CSF Aβ42 may be stronger in gray and white matter areas that are close to CSF spaces. This suggests that the degree to which CSF Aβ42 levels can be considered as a peripheral indicator of β-amyloid pathology depends on the localization of β-amyloid deposition in the brain. In accord with this view, it has been demonstrated that the clearance of Aβ42 from the brain is location-dependent. The results of the present study also caution against using CSF Aβ42 levels for the staging of AD pathology.

Supplementary Material

Refer to Web version on PubMed Central for supplementary material.

Acknowledgments

This work was supported in part by the German research foundation (Deutsche Forschungsgemeinschaft) Project Number: HE 4560/1-2 (AD, GH, HJW), DR 445/3-1 (AD), DR 445/4-1 (AD); by a Kommission Klinische Forschung Grant for clinical research of the Technische Universität München (AD, TG); and by the National Institutes of Health: R01 AG018402 (CAM), R37 AG025516 (WEK), P01 AG025204 (WEK).

GE Healthcare (formerly Amersham Health, Chalfont St. Giles, United Kingdom) entered into a license agreement with the University of Pittsburgh based on some of the technology described in this article. Prof. Dr. W. E. Klunk and Prof. C. A. Mathis are coinventors of carbon-11-labeled Pittsburgh Compound B ([^{11}C]PiB) and, as such, have a financial interest in this license agreement. The other authors, i.e., Dr. T. Grimmer, Dr. M. Riemenschneider, Prof. Dr. H. Förstl, Prof. Dr. G. Henriksen, Dr. T. Shiga, Prof. H. Wester, Prof. Dr. A. Kurz, and Dr. A. Drzezga reported no biomedical financial interests or potential conflicts of interest relevant to the subject matter of the manuscript.

References

1. Braak H, Braak E. Neuropathological stageing of Alzheimer-related changes. Acta Neuropathol 1991;82:239 –259. [PubMed: 1759558]
2. Thal DR, Rüb U, Orantes M, Braak H. Phases of Aβ-deposition in the human brain and its relevance for the development of AD. Neurology 2002;58:1791–1800. [PubMed: 12084879]
3. Bailey P. Biological marker in Alzheimer's disease. Can J Neurol Sci 2007;34:72–76.
4. Hampel H, Teipel SJ, Fuchsberger T, Andreasen N, Wiltfang J, Otto M, et al. Value of CSF beta-amyloid1-42 and tau as predictors of Alzheimer's disease in patients with mild cognitive impairment. Mol Psychiatry 2004;9:705–710. [PubMed: 14699432]
5. Riemenschneider M, Lautenschlager N, Wagenpfeil S, Diehl J, Drzezga A, Kurz A. Cerebrospinal fluid tau and β-Amyloid 42 proteins identify Alzheimer disease in subjects with mild cognitive impairment. Arch Neurol 2002;59:1729 –1734. [PubMed: 12433260]
6. Moonis M, Swearer JM, Dayaw MP, St George-Hyslop P, Rogaeva E, Kawarai T, Pollen DA. Familial Alzheimer disease: Decreases in CSF Aβ42 levels precede cognitive decline. Neurology 2005;65:323–325. [PubMed: 16043812]
7. Hulstaert F, Blennow K, Ivanoiu A, Schoonderwaldt HC, Riemenschneider M, De Deyn PP, et al. Improved discrimination of AD patients using β-amyloid (1-42) and tau levels in CSF. Neurology 1999;52:1555–1562. [PubMed: 10331678]

8. Sunderland T, Linker G, Mirza N, Putnam KT, Friedman DL, Kimmel LH, et al. Decreased β-amyloid 1-42 and increased tau levels in cerebrospinal fluid of patients with Alzheimer disease. JAMA 2003;289:2094 –2103. [PubMed: 12709467]
9. de Jong D, Kremer BPH, Olde Rikkert MGM, Verbeek MM. Current state and future directions of neurochemical biomarkers for Alzheimer's disease. Clin Chem Lab Med 2007;45:1421–1434. [PubMed: 17970699]
10. Riemenschneider M, Schmolke M, Lautenschlager N, Vanderstichele H, Vanmechelen E, Guder WG, Kurz A. Association of CSF apolipoprotein E, Aβ 42 and cognition in Alzheimer's disease. Neurobiol Aging 2002;23:205–211. [PubMed: 11804704]
11. Weller RO. How well does the CSF inform upon pathology in the brain in Creutzfeldt-Jakob and Alzheimer's diseases? J Pathol 2001;194:1–3. [PubMed: 11329133]
12. Strozyk D, Blennow K, White LR, Launer LJ. CSF Aβ 42 levels correlate with amyloid-neuropathology in a population-based autopsy study. Neurology 2003;60:652– 656. [PubMed: 12601108]
13. Tapiola T, Pirttilä T, Mikkonen M, Mehta PD, Alafuzoff I, Koivisto K, Soininen H. Three-year follow-up of cerebrospinal fluid tau, β-amyloid 42 and 40 concentrations in Alzheimer's disease. Neurosci Lett 2000;280:119 –122. [PubMed: 10686392]
14. Blennow K, Hampel H. CSF markers for incipient Alzheimer's disease. Lancet Neurol 2003;2:605–613. [PubMed: 14505582]
15. Sotthibundhu A, Sykes AM, Fox B, Underwood CK, Thangnipon W, Coulson EJ. β-Amyloid1-42 induces neuronal death through the p75 neurotrophin receptor. J Neurosci 2008;28:3941–3946. [PubMed: 18400893]
16. de Leon MJ, Mosconi L, Blennow K, DeSanti S, Zinkowski R, Mehta PD, et al. Imaging and CSF studies in the preclinical diagnosis of Alzheimer's disease. Ann N Y Acad Sci 2007;1097:114 –145. [PubMed: 17413016]
17. Klunk WE, Engler H, Nordberg A, Wang Y, Blomqvist G, Holt DP, et al. Imaging brain amyloid in Alzheimer's disease with Pittsburgh Compound-B. Ann Neurol 2004;55:306 –319. [PubMed: 14991808]
18. Ikonomovic MD, Klunk WE, Abrahamson EE, Mathis CA, Price JC, Tsopelas ND, et al. Post-mortem correlates of in vivo PiB-PET amyloid imaging in a typical case of Alzheimer's disease. Brain 2008;131:1630 –1645. [PubMed: 18339640]
19. Lockhart A, Lamb JR, Osredkar T, Sue LI, Joyce JN, Ye L, et al. PIB is a non-specific imaging marker of amyloid-beta (Aβ) peptide-related cerebral amyloidosis. Brain 2007;130:2607–2615. [PubMed: 17698496]
20. Fodero-Tavoletti MT, Smith DP, McLean CA, Adlard PA, Barnham KJ, Foster LE, et al. In vitro characterization of Pittsburgh compound-B binding to Lewy bodies. J Neurosci 2007;27:10365–10371. [PubMed: 17898208]
21. Fagan AM, Mintun MA, Mach RH, Lee SY, Dence CS, Shah AR, et al. Inverse relation between in vivo amyloid imaging load and cerebrospinal fluid Abeta42 in humans. Ann Neurol 2006;59:512–519. [PubMed: 16372280]
22. Drzezga A, Grimmer T, Henriksen G, Stangier I, Perneczky R, Diehl-Schmid J, et al. Imaging of amyloid plaques and cerebral glucose metabolism in semantic dementia and Alzheimer's disease. Neuroimage 2008;39:619 – 633. [PubMed: 17962045]
23. Engler H, Forsberg A, Almkvist O, Blomquist G, Larsson E, Savitcheva I, et al. Two-year follow-up of amyloid deposition in patients with Alzheimer's disease. Brain 2006;129:2856 –2866. [PubMed: 16854944]
24. Folstein MF, Folstein SE, McHugh PR. 'Mini Mental State'. A practical method for grading the cognitive state of patients for the clinician. J Psychiatr Res 1975;12:189 –198. [PubMed: 1202204]
25. Morris JC, Heyman A, Mohs RC, Hughes JP, van Belle G, Fillenbaum G, et al. The Consortium to Establish a Registry for Alzheimer's Disease (CERAD). Part I. Clinical and neuropsychological assessment of Alzheimer's disease. Neurology 1989;39:1159 –1165. [PubMed: 2771064]
26. McKhann G, Drachman D, Folstein M, Katzman R, Price D, Stadlan EM. Clinical diagnosis of Alzheimer's disease: Report of the NINCDS-ADRDA Work Group under the auspices of Department

of Health and Human Services Task Force on Alzheimer's Disease. Neurology 1984;34:939–944. [PubMed: 6610841]

27. Minoshima S. Imaging Alzheimer's disease: Clinical applications. Neuroimaging Clin N Am 2003;13:769 –780. [PubMed: 15024960]
28. Román GC, Tatemichi TK, Erkinjuntti T, Cummings JL, Masdeu JC, Garcia JH, et al. Vascular dementia: Diagnostic criteria for research studies. Report of the NINDS-AIREN International Workshop. Neurology 1993;43:250 –260. [PubMed: 8094895]
29. Zivelin A, Rosenberg N, Peretz H, Amit Y, Kornbrot N, Seligsohn U. Improved method for genotyping apolipoprotein E polymorphisms by a PCR-based assay simultaneously utilizing two distinct restriction enzymes. Clin Chem 1997;43:1657–1659. [PubMed: 9299950]
30. Vandermeeren M, Mercken M, Vanmechelen E, Six J, van de Voorde A, Martin JJ, Cras P. Detection of tau proteins in normal and Alzheimer's disease cerebrospinal fluid with sensitive sandwich enzyme-linked immunosorbent assay. J Neurochem 1993;61:1828 –1834. [PubMed: 8228996]
31. Friston KJ, Frith CD, Liddle PF. The relationship between global and local changes in PET scans. J Cereb Blood Flow Metab 1990;10:458 – 466. [PubMed: 2347879]
32. Grimmer T, Diehl J, Drzezga A, Förstl H, Kurz A. Region-specific decline of cerebral glucose metabolism in patients with frontotemporal dementia: A prospective 18F-FDG-PET study. Dement Geriatr Cogn Disord 2004;18:32–36. [PubMed: 15084791]
33. Lopresti BJ, Klunk WE, Mathis CA, Hoge JA, Ziolko SK, Lu X, et al. Simplified quantification of Pittsburgh Compound B amyloid imaging PET studies: A comparative analysis. J Nucl Med 2005;46:1959 –1972. [PubMed: 16330558]
34. Ziolko SK, Weissfeld LA, Klunk WE, Mathis CA, Hoge JA, Lopresti BJ, et al. Evaluation of voxel-based methods for the statistical analysis of PIB PET amyloid imaging studies in Alzheimer's disease. Neuroimage 2006;33:94 –102. [PubMed: 16905334]
35. Grimmer T, Henriksen G, Wester HJ, Förstl H, Klunk WE, Mathis CA, et al. Clinical severity of Alzheimer's disease is associated with PIB uptake in PET [published online ahead of print March 16]. Neurobiol Aging. 2008
36. Tzourio-Mazoyer N, Landeau B, Papathanassiou D, Crivello F, Etard O, Delcroix N, et al. Automated anatomical labeling of activations in SPM using a macroscopic anatomical parcellation of the MNI MRI single-subject brain. Neuroimage 2002;15:273–289. [PubMed: 11771995]
37. Loening AM, Gambhir SS. AMIDE: A free software tool for multimodality medical image analysis. Mol Imaging 2003;2:131–137. [PubMed: 14649056]
38. Friston KJ, Holmes AP, Worsley KJ. Statistical Parametric Mapping in functional imaging: A general linear approach. Hum Brain Mapp 1995;2:189 –210.
39. Talairach, J.; Tournoux, P. Co-planar Stereotactical Atlas of the Human Brain: 3-Dimensional Proportional System–An Approach to Cerebral Imaging. Stuttgart, Germany: Georg Thieme Verlag; 1988.
40. Engelborghs S, Sleegers K, Cras P, Brouwers N, Serneels S, De Leenheir E, et al. No association of CSF biomarkers with APOEe4, plaque and tangle burden in definite Alzheimer's disease. Brain 2007;130:2320 –2326. [PubMed: 17586559]
41. Thal DR, Capetillo-Zarate E, Del Tredici K, Braak H. The development of amyloid beta protein deposits in the aged brain. Sci Aging Knowledge Environ 2006:re1. [PubMed: 16525193]
42. Weller RO, Subash M, Preston SD, Mazanti I, Carare RO. Perivascular drainage of amyloid-beta peptides from the brain and its failure in cerebral amyloid angiopathy and Alzheimer's disease. Brain Pathol 2008;18:253–266. [PubMed: 18363936]
43. Weller RO. Pathology of cerebrospinal fluid and interstitial fluid of the CNS: Significance for Alzheimer disease, prion disorders and multiple sclerosis. J Neuropathol Exp Neurol 1998;57:885–894. [PubMed: 9786239]
44. Zhang ET, Richards HK, Kida S, Weller RO. Directional and compartmentalised drainage of interstitial fluid and cerebrospinal fluid from the rat brain. Acta Neuropathol 1992;83:233–239. [PubMed: 1373020]
45. Edison P, Rowe CC, Rinne JO, Ng S, Ahmed I, Kemppainen N, et al. Amyloid load in Parkinson's disease dementia and Lewy body dementia measured with [11C]PIB positron emission tomography. J Neurol Neurosurg Psychiatry 2008;79:1331–1338. [PubMed: 18653550]

46. Gomperts SN, Rentz DM, Moran E, Becker JA, Locascio JJ, Klunk WE, et al. Imaging amyloid deposition in Lewy body diseases. Neurology 2008;71:903–910. [PubMed: 18794492]

47. McKeith IG, Galasko D, Kosaka K, Perry EK, Dickson DW, Hansen LA, et al. Consensus guidelines for the clinical and pathologic diagnosis of dementia with Lewy bodies (DLB): Report of the Consortium on DLB International Workshop. Neurology 1996;47:1113–1124. [PubMed: 8909416]

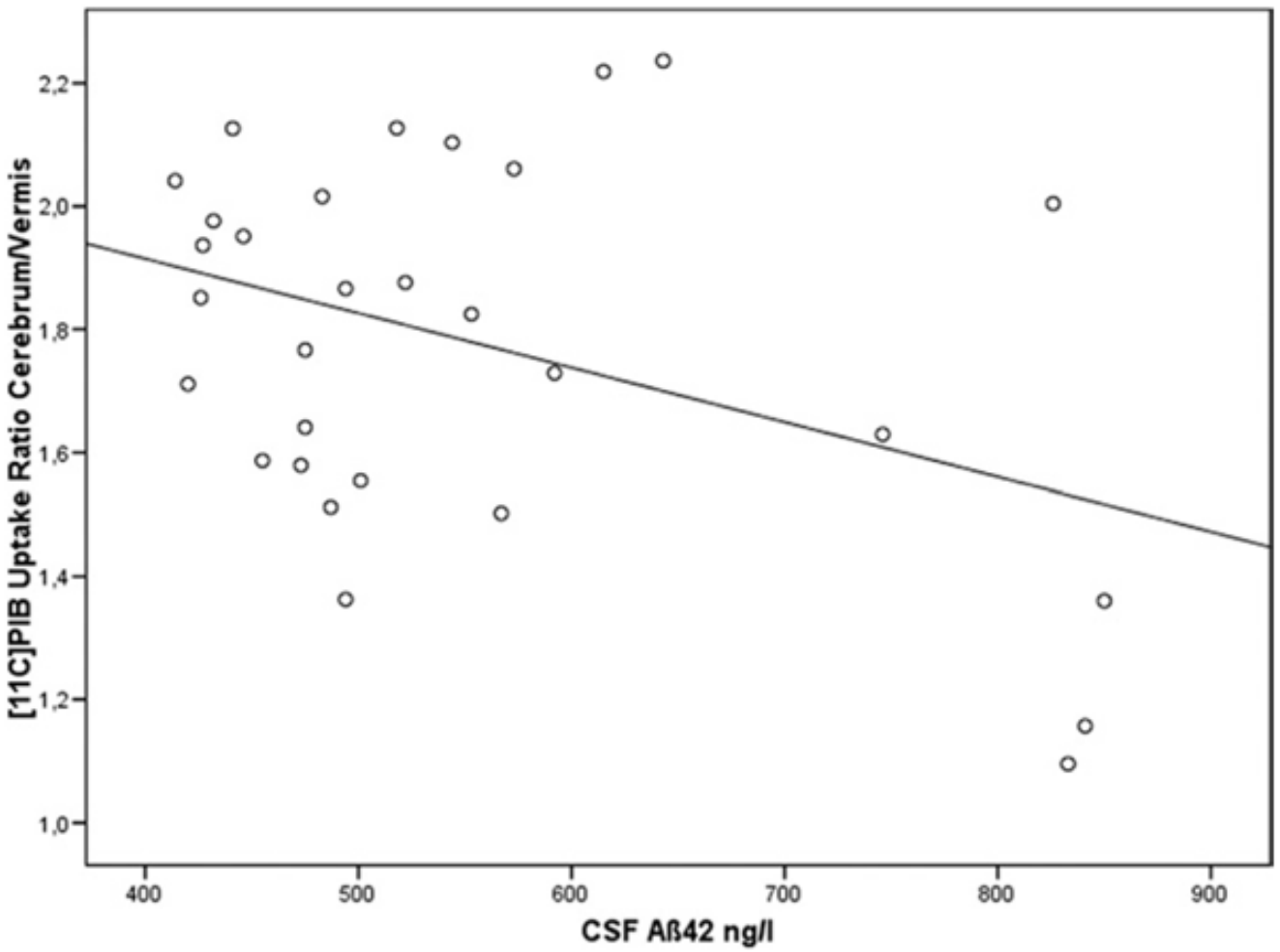

Figure 1.
Linear regression analysis between [^{11}C]PiB cerebrum/vermis uptake ratio and CSF Aβ42. Standardized regression coefficient Beta = −0,478; p = .01. Aβ42, beta amyloid [1-42]; [^{11}C] PiB, carbon-11-labeled Pittsburgh Compound B; CSF, cerebrospinal fluid.

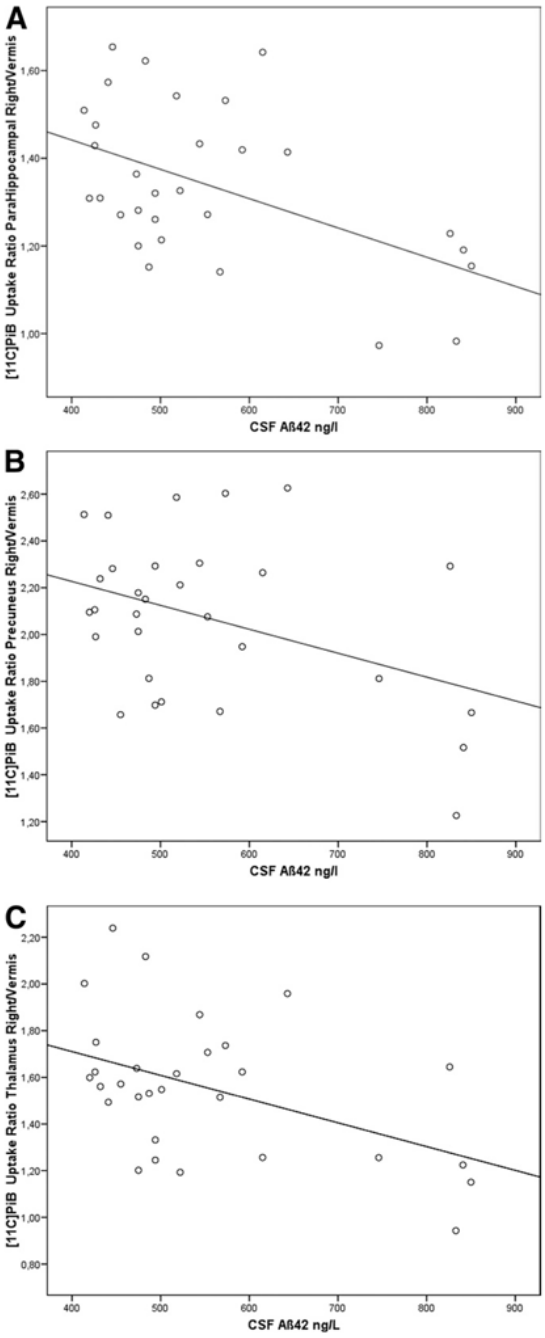

Figure 2.

Correlation analyses between [^{11}C]PiB cerebrum/vermis uptake ratios and CSF Aβ42 in anatomically defined regions of interest. Correlation coefficients (Pearson): **(A)** $r = -.503$, $p = .005$; **(B)** $r = -.400$, $p = .029$; **(C)** $r = -.460$, $p = .011$. Aβ42, beta amyloid [1-42]; [^{11}C]PiB, carbon-11-labeled Pittsburgh Compound B; CSF, cerebrospinal fluid.

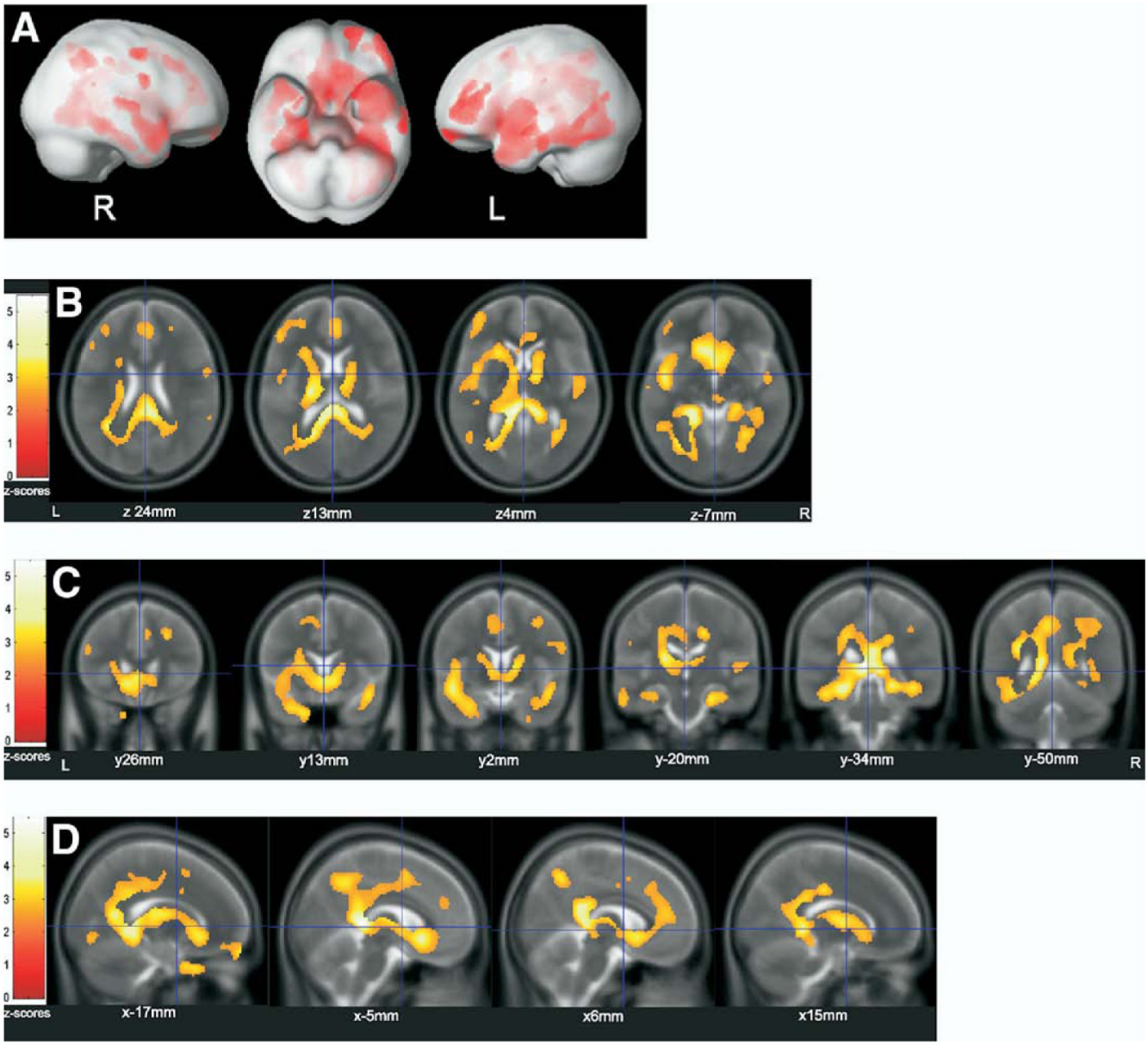

Figure 3.

Voxel-based regression analysis between [^{11}C]PiB uptake and CSF Aβ42. Significant ($p < .01$) associations: **(A)** projected to the surface; **(B–D)** overlaid on T2-scans (average of 152 scans, implemented in SPM2). **(B)** axial, **(C)** coronal, **(D)** saggital. Aβ42, beta amyloid [1-42]; [^{11}C]PiB, carbon-11-labeled Pittsburgh Compound B; CSF, cerebrospinal fluid; L, left; R, right; x/y/z, coordinates of slices in Talairach space.

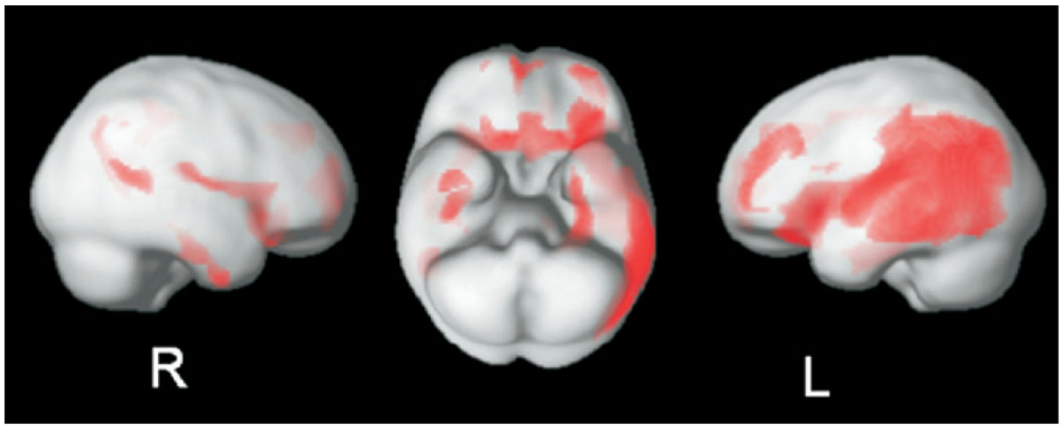

Figure 4.
Partial volume effect corrected voxel-based regression analysis between [^{11}C]PiB uptake and CSF Aβ42. Significant ($p < .01$) associations projected to the surface. Aβ42, beta amyloid [1-42]; [^{11}C]PiB, carbon-11-labeled Pittsburgh Compound B; CSF, cerebrospinal fluid; L, left; R, right.

Table 1

Patients' Clinical and Demographic Characteristics

Number	30
Male : Female	20 : 10
APOE ε 4 Alleles: 0 : 1 : 2	11 : 11 : 8
Age (mean/standard deviation) in Years	66.8 ± 8.0 (range 51–82)
Duration of Disease in Years	3.2 ± 2.1 (range 0–9)
CDR SOB (mean/standard deviation)	4.2 ± 2.6 (range .5–11)
MMSE (mean/standard deviation)	23.1 ± 4.7 (range 11–30)
CSF Aβ42 (mean/standard deviation) in ng/L	552.3 ± 135.5 (range 414–850)

(Aβ42), beta amyloid (1–42); APOE, apolipoprotein E; CDR SOB, Clinical Dementia Rating Sum of Boxes; CSF, cerebrospinal fluid; MMSE, Mini Mental State Examination.